Effect of Laminate Properties on the Failure of Cross Arm Structure under Multi-Axial Load

IOP Conf. Series: Materials Science and Engineering **530** (2019) 012029 doi:10.1088/1757-899X/530/1/012029

Effect of Laminate Properties on the Failure of Cross Arm Structure under Multi-Axial Load

D Mohamad[1], A Syamsir[2], S Beddu[1], N L M Kamal[1], M M Zainoodin[1], M F Razali[3]*, A Abas[3], S A H A Seman[3] and F C Ng[3]

[1] Department of Civil Engineering, Universiti Tenaga Nasional, 43000 Kajang, Malaysia.

[2] Institute of Energy Infrastructures (IEI), Universiti Tenaga Nasional, 43000 Kajang, Malaysia.

[3] School of Mechanical Engineering, Universiti Sains Malaysia, Engineering Campus, 14300, Nibong Tebal, Penang, Malaysia.

Corresponding author *: mefauzinizam@usm.my

Abstract. This study investigated the influence of laminate properties toward the collapse of composite cross arm structure under multi-axial quasi-static loading. A three-dimensional finite-element model of a cross arm was developed and integrated with Hashin's failure subroutine to predict the inter-laminar damages of the composite upon its application. The mechanical deformation and failure of the composite structure were evaluated over three laminate properties. This investigation revealed that variation in laminates properties yielded different structural deflection and laminate damages. The cross arm with a greater young modulus and ultimate stresses (laminate B) experienced a single failure mode of fiber buckling in compression at deflection of 0.082 m. For the given multi-axial load, the laminate configuration and properties considered in this study failed to prevent the failure of the cross arm.

1. Introduction

Through years, demand for a stiffer, stronger and lighter laminated composite has grown in many fields such as aerospace, energy and civil construction. For laminated composites made of unidirectional layers, the best performance can be achieved provided that the applied loading direction matches with the reinforcement direction. However, this condition is hard to realize in real application as the loading scenarios are often multiaxial. For such applications, employing laminated composites made of unidirectional layers may provide a poor solution.

Additionally, improper laminated composites are also prone to mechanical damages when they are exposed to various types of loadings such as compressive, tension, and flexural which can lead to material failure [1]. In order to improve the use of laminated composites for high load applications, it is important to understand the mechanical and damage behavior of laminated composite under multidirectional loadings. The best method to refine the damage-resistance characteristics of laminated composites is to use an appropriate combination of fiber orientations, plies thickness, adequate number of laminates and properties that exactly fit the requirement for a particular purpose [2].

Finite-element method has been widely used to study and predict the damage behavior of laminated structures through the implementation of different failure criteria [3-4]. The early generation of failure criteria was based on those criteria developed for isotropic materials, such as von Mises

criterion. Unfortunately, most of these early developed criteria are not associated to any type of failure mode. In recent years, Hashin criterion [5] was extensively considered for composite related problems as it associated with different types of failure modes, in specific fiber buckling and matrix cracking.

The purpose of this study is to evaluate the failure modes of different laminate properties cross arms under quasi-static loading condition. The study was conducted using a computational techniques by developing a three-dimensional finite-element model that simulated the standard configuration of cross arm installed on a transmission tower. The failure of cross arm upon loading was evaluated by Hashin's failure criteria, which being employed through user subroutine. The analysis focused on the structural deflection, and the intra-laminar damages exhibited by the cross arm during the application of static load at one end. This finding may assist engineers in selecting the best laminate properties to comply with the severe multi-axial load condition experienced by the composite cross arm.

2. Description of numerical models

2.1 Geometry, mesh and boundary conditions

In this section, the generation of the finite-element models are described following the scope of Abaqus commercial package. A numerical cross arm model was developed by using the finite-element analysis software program Abaqus/CAE. The analysis was carried out with explicit solver, and this solver was selected for quasi-static modeling due to high computational time needed for the whole model analysis. A proper combination of loading rates and mass scaling methods have been applied to reduce the computational time of the explicit time integration method [6].

As shown in Figure 1, the cross arm model consists of four square (0.12 x 0.12 mm^2) composite beam with a length of 4.9 m. The square beam composed 7 stacked plies of glass laminate, each ply having a 1.0 mm thickness. The stacking sequences of the beam are [45/ -45/ 0/ 90/ 0/ 90/ 0]. The cross arm model was modeled by using a total of 73472 linear hexahedral element with reduced integration (C3D8R). The end of the cross arm was loaded with a longitudinal force (F_l) of 6524 N, a vertical downward force (F_v) of 84992 N and a transverse force (F_t) of 46416 N. These force magnitudes reflect the weight of power lines hanged between the cross arms (multiplied by a safety factor of four). The other ends of the cross arm were constrained to be fixed in all directions (encastre).

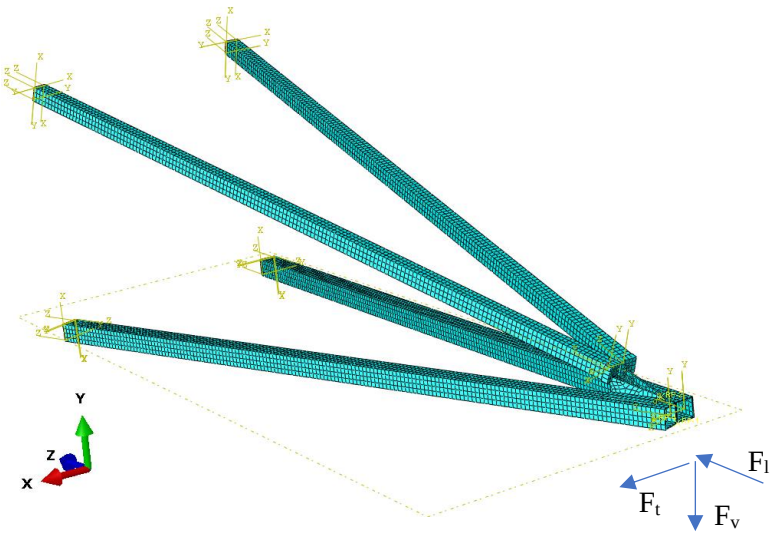

Figure 1. Geometry and mesh of the finite-element model of composite cross arm.

The possible location of the contact between the layer surfaces was defined by surface-to-surface discretization, with a normal contact defined as "hard". For the analysis output, the user-dependent state variable (SDV 1 to SDV 4) was requested from the numerical simulation as these variables represent

the failure modes of fiber breakage in tension, fiber buckling in compression, matrix cracking in tension and matrix crushing in compression, respectively. Additionally, the deflection (U) of the whole model was also requested for comparison.

2.2 Material properties

The material that constitutes each ply of the cross arm is a glass laminate. The provided mechanical properties of each laminate are presented in Table 1. Three laminate properties, in specific, laminate A, B and C were considered to evaluate the structural deformation of the cross arm. It is worth noting that small difference in laminate properties was recognized between laminate A and C, while greater young modulus and ultimate stresses was recorded for laminate B. This input of material properties was assigned by means of the *USER MATERIAL instruction in Abaqus framework.

Table 1. Mechanical properties of laminate A, B and C.

No.	Parameter	Laminate A	Laminate B	Laminate C
1	Density	1.8 g/cm^3	1.9 g/cm^3	1.8 g/cm^3
2	Young's modulus, E_1	16000 MPa	36300 MPa	17000 MPa
3	Young's modulus, E_2	4800 MPa	10890 MPa	5100 MPa
4	Young's modulus, E_3	1440 MPa	3267 MPa	1530 MPa
5	Poisson's ratio (V_{12}=V_{13}=V_{23})	0.28	0.28	0.28
6	Shear modulus (G_{12}=G_{13}=G_{23})	4000 MPa	4000 MPa	4000 MPa
7	Ultimate tensile stress, X_{1T}	321 MPa	429 MPa	321 MPa
8	Ultimate compressive stress, X_{1C}	150 MPa	320 MPa	150 MPa
9	Ultimate tensile stress, X_{2T}	80 MPa	100 MPa	80 MPa
10	Ultimate compressive stress, X_{2C}	65 MPa	76 MPa	65 MPa
11	Ultimate shear stress, S_{12}	90 MPa	95 MPa	89 MPa
12	Ultimate shear stress, (S_{13} = S_{23})	60 MPa	70 MPa	50 MPa

2.3 Failure criteria

A VUMAT/Hashin subroutine was employed to predict the breaking of the fibers and the progressive damage in the matrix of the cross arm. The Hashin failure criterion is based on the work of Hashin [5]. Unlike the polynomial criteria such as the Tsai-Wu criteria [7], which propose a single equation to predict damage initiation, Hashin damage initiation criterion takes into account four possible failure modes. The four possible failure modes are fiber breakage in tension, fiber buckling in compression, matrix cracking in tension and matrix crushing in compression. Equation 1 to 4 were used to predict the previous failure modes respectively, and failure is expected when one of the following equations is satisfied (equivalent to 1).

$$(\frac{\sigma_{11}}{X_{1T}})^2+(\frac{\sigma_{12}}{S_{12}})^2+(\frac{\sigma_{13}}{F_{13}})^2=1 \quad (1)$$

$$(\frac{\sigma_{11}}{X_{1C}})^2=1 \quad (2)$$

$$\frac{(\sigma_{22}+\sigma_{33})^2}{X_{2t}^2}+\frac{\sigma_{23}-\sigma_{22}\sigma_{33}}{S_{23}^2}+\frac{\sigma_{12}^2+\sigma_{13}^2}{S_{12}^2}=1 \quad (3)$$

$$\left[\left(\frac{X_{2c}}{2S_{23}}\right)-1\right]\frac{(\sigma_{22}+\sigma_{33})}{X_{2c}}+\frac{(\sigma_{22}+\sigma_{33})^2}{4S_{23}^2}+\frac{(\sigma_{23}^2-\sigma_{22}\sigma_{33})}{S_{23}^2}]+\frac{\sigma_{12}^2+\sigma_{13}^2}{S_{12}^2}=1 \quad (4)$$

where σ_{11}, σ_{22}, σ_{33}, σ_{12}, σ_{13} and σ_{23} are the applied stresses.

3. Result and discussion

Table 2 summarizes the deflection and failure mode of the numerical model for the three laminate properties. The maximum deflection indicates the highest deflection allows before failure started to occur on the finite-element model. It is seen that laminate C recorded the highest deflection of 0.187 m, followed by laminate A and B. The small deflection recorded with laminate B is related to its higher young modulus, especially for the first direction (E_1). This high young modulus of laminate B cause the cross arm to be a lot stiffer, hence resulting to a smaller deflection for a given bending load.

Additionally, it is worth noting that every laminate properties considered in this study lead to a failure of the cross arm model. The value 1 recorded in Table 2 indicates that the damage initiation criterion was met. It is recognized that both laminate A and C exhibited fiber breakage due to tension (SDV 1) and fiber buckling due to compression (SDV 2). Interestingly, since laminate B result to a smaller deflection upon the loading, only failure due to fiber buckling in compression was recorded.

Table 2. Deflection and failure modes of cross arm of different laminate properties.

No.	Parameter	Laminate A	Laminate B	Laminate C
1	Maximum deflection (m)	0.174	0.082	0.187
2	Fiber breakage in tension (SDV 1)	1	0	1
3	Fiber buckling in compression (SDV 2)	1	1	1
4	Matrix cracking in tension (SDV 3)	0	0	0
5	Matrix crushing in compression (SDV 4)	0	0	0

Figure 2 shows the failure of fiber in compression (SDV 2) of the cross arm for laminate A, B and C. There are two dominant colors can be seen; the blue color indicates the region which free from failure and the red region highlight a region with fiber buckling. It is observed that despite the variation in laminate properties, each case exhibited the failure on similar location, which localized nearly at the middle region of the lower beams. This observation also highlighted that throughout the application of the load, the lower beams experienced greater bending deformation than the upper beams.

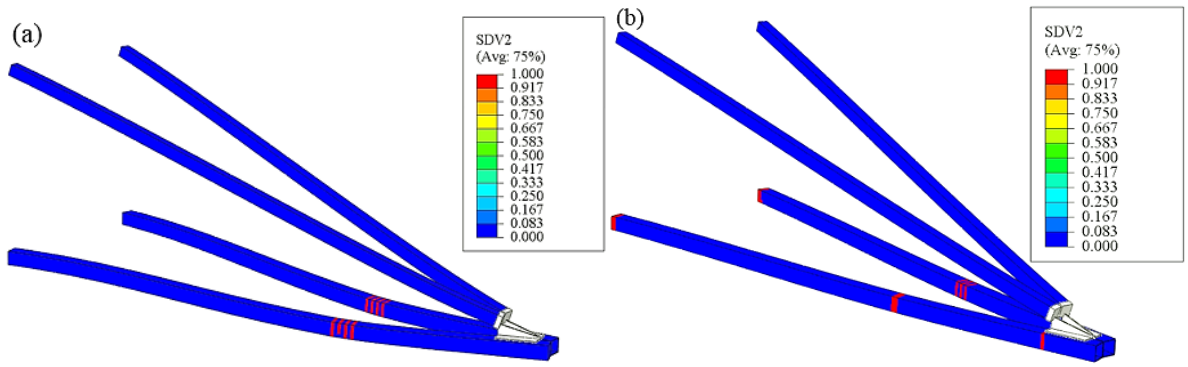

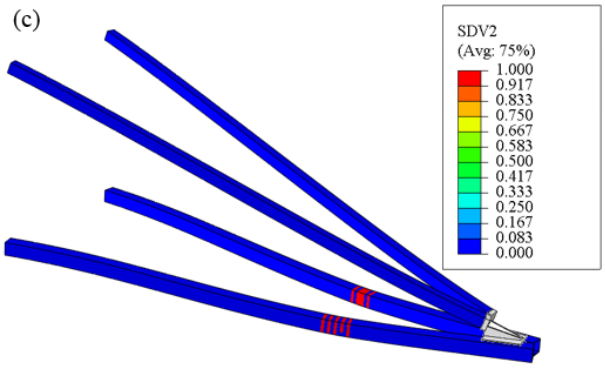

Figure 2. Failure location due to fiber buckling in compression (SDV 2): (a) laminate A, (b) laminate B and (c) laminate C.

4. Conclusion

The implementation of VUMAT/Hashin with finite element enabled the prediction of inter-laminar damages of a composite cross arm. A variation in laminate properties of the cross arm yielded different bending deflection and modes of failure. A cross arm with greater value of young modulus and ultimate stresses (laminate B) exhibited smaller deflection and lesser number of failures upon subjected to multi-axial load condition.

Acknowledgement:

TNB Seeding Fund funds this research for Universiti Tenaga Nasional (U-T-S-RD-17-05). The authors would like to thank TNB Transmission Line Division and TNB for financial support.

References:

[1] N Jauhari, R Mishra and H Thakur 2017 Failure Analysis of Fibre-Reinforced Composite Laminates *Mater. Today Proc.* Vol 4 No 2 Part A pp 2851–2860

[2] F S Almeida and A M Awruch 2009 Design optimization of composite laminated structures using genetic algorithms and finite element analysis *Compos. Struct.* Vol 88 No 3 pp 443–454

[3] Wang Gong-Dong, Melly Stephen Kirwa and Ahmed S K Kafi 2018 Finite element study into the effects of fiber orientations and stacking sequence on drilling induced delamination in CFRP/Al stack *Science and Engineering of Composite Materials* Vol 25 p 555

[4] J Ye, Y Yan, J Li, Y Hong and Z Tian 2018 3D explicit finite element analysis of tensile failure behavior in adhesive-bonded composite single-lap joints *Compos. Struct.* Vol 201 pp 261–275

[5] Z Hashin Jun 1980 Failure Criteria for Unidirectional Fiber Composites *J. Appl. Mech.* Vol 47 No 2 pp 329–334

[6] J Wang, T Chen, D Sleight and A Tessler 2004 Simulating nonlinear deformations of solar sail membranes using explicit time integration in *45th AIAA/ASME/ASCE/AHS/ASC Structures, Structural Dynamics & Materials Conference* p 1580

[7] S W Tsai and E M Wu 1971 A General Theory of Strength for Anisotropic Materials *J. Compos. Mater.* Vol 5 No 1 pp 58–80